Thermal shocks and magnetohydrodynamics in high power mercury jet targets

J Lettry†, A Fabich†, S Gilardoni†, M Benedikt†, M Farhat¶and E Robert¶

† CERN, CH-1211 Geneva 23

¶ Swiss Federal Institute of Technology (EPFL), Laboratory For Hydraulic Machines Lausanne (LMH), Switzerland

E-mail: `jacques.lettry@cern.ch`

Abstract. The response of mercury samples submitted to a pulsed proton beam and the magneto-hydrodynamic (MHD) effects of a mercury jet injected into a 20 Tesla magnetic field are reported. The experimental conditions differ from those of proposed neutrino factories [1, 2] and the purpose of these measurements is to provide benchmarks for simulation tools of a realistic free mercury jet target. These measurements were completed in June 2002. Analysis is ongoing and the presented results are preliminary.

Submitted to: *J. Phys. G: Nucl. Phys.*

PACS numbers: n.a.

1. Proton induced thermal shock in mercury

Pulsed proton beam induced effects were already observed in contained molten metal targets (Pb, Sn, La) [3]. A proton pulse of only $2\text{x}10^{12}$ protons (24 GeV) leads to the disruption of a free mercury jet [4] while neutrino factory pulse intensities are one to two orders of magnitude higher. The response (in terms of splash velocities) of a $1\,\text{cm}^3$ mercury sample contained in a stainless steel thimble to proton pulse intensities up to $30\text{x}10^{12}$ (1.4 GeV) protons is reported in [5] and confirms the expected scaling with the temperature elevation [6] as well as the reduction of the splashing for a proton pulse duration larger than the relaxation time scale of the sample (sample size/speed of sound). A $7\,\text{cm}^3$ mercury sample contained in a stainless steel trough with a length of 60 mm (Figure 1) was submitted to the CERN PS-Booster proton beam within the ISOLDE target area. The experimental setup consists of a high-speed camera recording the shadow of mercury droplets intercepting a parallel light beam. The resolution of the high-speed camera, placed behind a concrete shielding at a distance of 10 m was 0.77 mm per pixel. Obviously, small droplets such as the high velocity ones observed in [4] with a different camera and a laser light source, different mirror optics and a shorter observation distance are not visible.
At first glance, the scaling observations made with the thimble are reproduced. As an example, the response of the mercury contained in a trough irradiated with $20\text{x}10^{12}$ protons (1.4 GeV) was measured by monitoring the height of the mercury droplets expelled from the trough and is presented in Figure 2. The energy deposited by the proton pulse into the mercury sample was computed using MARS [8] interfaced with MCNP4C [9]). The maximum temperature elevation amounts to 250 K. The predicted proportionality of the initial velocity to the temperature elevation is confirmed within the precision of the measurement over the length of the trough. Indeed, the computed energy deposition and the splash velocity profile presented in Figure 2 show similar profiles.
The proton induced splashing observed in the free jet [4] could be generated by the propagating compression shock wave immediately following the energy deposition. Could the observed splashing be the result of the shock wave generated by a collapsing vapour bubble (signature of cavitation) close to the free liquid surface? To address this point, the monitoring of the collapsing vapour bubble is simpler in transparent media. Cavitation is a well-studied phenomenon in the framework of its deleterious corrosion on piping or propellers. Such a material test setup where the vapourisation of water is induced by means of a spark discharge was modified to study cavitation in the vicinity of a free surface. Qualitative information was gained by recording with a digital camera the light of a flash transmitted through the liquid few millisecond after the spark. While the initial shock did not disrupt the surface of the liquid, a vapour bubble collapsing close to the surface did. In the picture presented in Figure 3 a thin jet is visible that has similarities with some of the proton induced splashes in mercury jets shown in [4]. In both cases, the energy deposited is of a few Joule. However, the influence of the type of

fluid, position and geometry of the spark gap or bubble has not yet been investigated. While the cavitation corrosion pattern was observed in contained lead targets [10], any conclusion about its appearance in free jets is premature. However, this investigation shall be continued. Vapour bubbles will be generated close to the free surface by a Neodim YAG laser to avoid the actual reflection of pressure waves on the electrodes and to reduce the heat deposition time from a few millisecond down to a fraction of the relaxation time (a few nanosecond).

The hydrodynamics of the free jet target requires a more specific analysis. A jet of mercury injected at a 25 m/s velocity within the 4 cm inner diameter of the magnetic horn [7] will be disrupted at 20 ms intervals over 30 cm. The resulting splashes will partially fill the volume and hit the confinement with radial splash velocities of 10 to 40 m/s. The flow of the disrupted mercury out of the horn must occur within 20 ms in order to avoid reabsorbing of the pions produced by the next proton pulse. Furthermore, the resilience to fatigue and corrosion under high radiation of the inner confinement of the jet submitted to a 50 Hz high velocity mercury splash should be addressed.

2. Magnetohydrodynamics

One of the high power target schemes proposed in [1] relies on a mercury jet injected with a velocity of ≈ 30 m/s under an angle of 6 degree into a 20 Tesla magnetic field. The 24 GeV proton pulse with a length of a few nanoseconds will interact with the target in the middle of the high field region and disrupt the jet as underlined in the previous section.

The MHD experiments were done at the Grenoble High Magnetic Field Laboratory (GHMFL). The field distribution of the M9 magnet is presented in Figure 4, the maximum field is 19.3 Tesla for a bore diameter of 130 mm and its axial distribution differs from the one of the pion collection staged magnet.

The test setup consists of a compressed air driven double piston pump feeding 4 mm inner diameter cylindrical nozzles. The maximum static pressure of the mercury is 90 bars and an air driven pneumatic valve placed 20 cm upstream from the nozzle is used to define the duration of the jet (typically $100-200$ ms). A stainless steel chamber sketched in Figure 4 is equipped with Plexiglas windows and sits between two mirrors placed at 90 degrees. The light of a 4 cm wide parallel laser beam is reflected by the first mirror, crosses the chamber and is reflected by the second mirror into the objective of the high speed camera that records the shadow of the jet. The pump, injector, valve, light source and mirrors are confined in a leak tested stainless steel confinement vessel equipped with an observation window. The mirrors can be moved along the chamber from the nozzle position to the bottom jet breaker. The confinement vessel is sitting on a lift that allows the positioning along the axis of the magnet coil. A piezo-electric pressure gauge is mounted at the beginning of the high-pressure piping to monitor the dynamic pressure losses of the moving mercury. The tungsten seats of the ceramic ball valves broke irremediable after typically 150 strokes. Beside pressure tests of the

plumbing and safety valves, the air leaving the safety enclosure is filtered.
Single frames from the film of the jet injected at an angle of 6 degree are presented in Figure 5. Calibration rulers are placed 1 cm apart on each side of the field axis. The tip of the jet and the jet itself recorded 10 ms after the passage of the tip are given for injection velocities between 8 and 11 m/s and a field strength of up to 19.3 Tesla. The injection of an 11 m/s mercury jet at an angle of 6 degree into a 20 Tesla field is successfully demonstrated. With increasing field, the smoothness of the jet envelope is clearly improved thus demonstrating the expected damping [12]. A 4 mm diameter jet injected in a 20 Tesla field stabilised at the desired injection angle within 10 ms. Minor misalignments or oscillation around the axis of the jet cannot be excluded. A larger jet such as the one proposed in neutrino factories would under similar conditions take more time to stabilise. It is not excluded that the nominal jet will stabilise into a cylindrical target within the 20 ms available between proton pulse induced disruptions. Jet velocities are presented in Figure 6 as a function of the magnetic field strength for different injection angles and initial pump pressure. The expected tendency for the velocity of the jet to be reduced with increasing field is observed. The reduction of the jet velocity is larger for a low velocity jet. At 20 Tesla, the velocity is reduced by typically 30%. However, MHD effects occurring in the piping and in the valve are specific of the experimental setup. Separation of these contributions requires a full MHD simulation of the injection circuit. Image processing and modelling will be published in [11].

Acknowledgments

The production and test of the setup prototypes greatly benefited from the help of E. Barbero, D. Carminati, N. Chritin and B. Crepieux. We thank F.Debray and E.Mossang from GHMFL for their support.

References

[1] Status of neutrino US-nufact scheme Feasibility Study-II of a Muon-Based Neutrino Source, ed., S. Ozaki, R. Palmer, M. Zisman, and J. Gallardo, BNL-52623, 2001 (http://www.cap.bnl.gov/mumu/studyii/FS2–report.html)
[2] The Study of a European Neutrino Factory Complex, P.Gruber (ed.) CERN/PS/2002-008.
[3] J. Lettry, R. Catherall, P. Drumm, A. Evensen, O.C. Jonsson, E. Kugler, J. Obert, J.C. Puteaux, J. Sauvage, M. Toulemonde and the ISOLDE Collaboration, ICANS-XIII, International Conference on Advanced Neutron Sources, PSI proceedings 95-02, 1995, 595.
[4] H.Kirk et al., Target Studies with BNL E951 at the AGS, proceedings PAC'01, Chicago, 2001
[5] A.Fabich, M.Benedikt, J.Lettry, Experimental Observation of Proton-Induced Shocks in Free Surface Liquid Metal Targets, proceedings IWSMT5, J.of Nuclear Materials, 2002, to be published
[6] P.Sievers, P. Pugnat, Response of Solid and Liquid Targets To High Power Proton Beams for Neutrino Factories, CERN-LHC/2000-4 (CERN-NuFACT Note 035), 2000
[7] S.Gilardoni, Status of a magntic horn for a neutrino factory, these proceedings
[8] N.V. Mokhov, "The Mars Code System User's Guide", Fermilab-FN-628 (1995). N.V. Mokhov, "MARS Code Developments, Benchmarking and Applications", Fermilab-Conf-00-066 (2000).

N.V. Mokhov, S.I. Striganov, A. Van Ginneken, S.G. Mashnik, A.J. Sierk and J. Ranft "MARS Code Developments", Fermilab-Conf-98/379 (1998); LANL Report LA-UR-98-5716 (1998); nucl-th/9812038 v2 16 Dec 1998.

O.E. Krivosheev and N.V. Mokhov, "A New MARS and its Applications", Fermilab-Conf-98/43 (1998).

[9] J.S. Hendrics, "MCNP4C" LANL Memo X-5; JSH-2000-3

J.F. Briesmesteir, ed. "MCNP - A General Montecarlo N-Particle Transport Code, Version 4C", LA-13709-M

[10] J.Lettry et al., Effects of Thermal Schocks on the Release of Radioisotopes and on Molten Metal Target Vessels, proc. EMIS-14, Canada, 2002

[11] A. Fabich, High Power Proton Beam Shocks and Magnetohydrodynamics in a Mercury Jet Target for a Neutrino Factory, CERN-THESIS-2002-038

[12] R. Samulyak, Numerical simulation of hydro- and magnetohydrodynamic processes in the Muon Collider target, Lecture Notes in Comp. Sci., Springer-Verlag, Berlin - Heidelberg, 2331 (1992), 391-400.

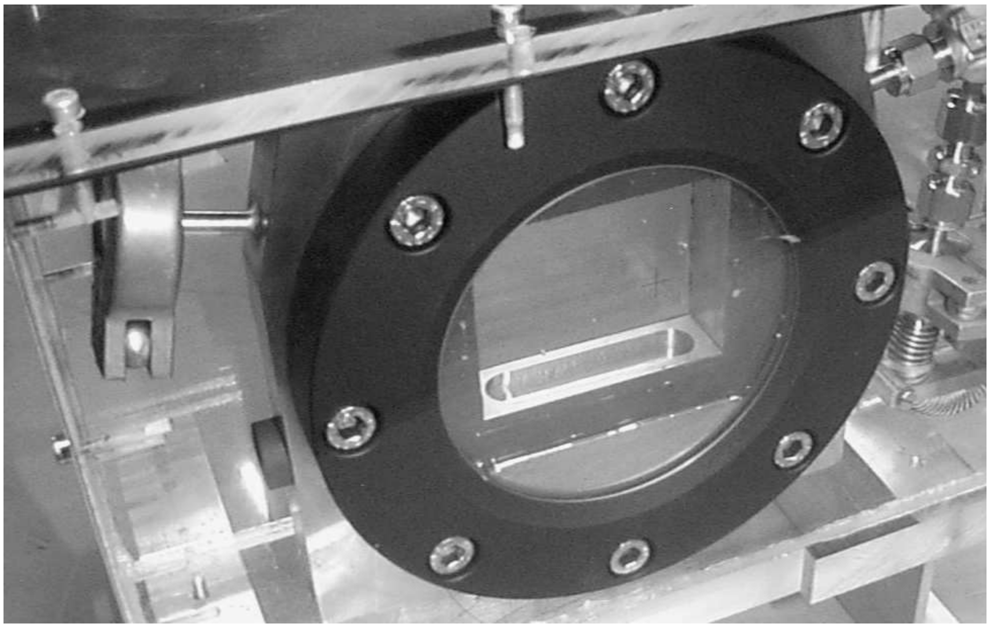

Figure 1. *Trough target. The trough is excavated in a steel frame, with the viewing windows on both sides. The steel frame is placed in a second confinement.*

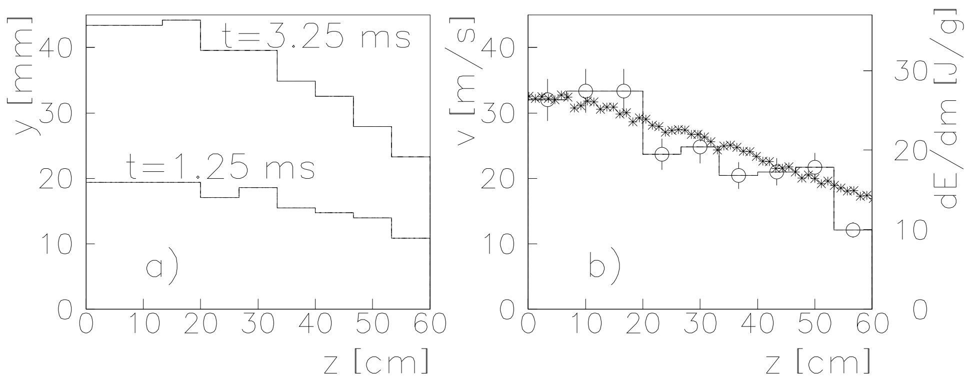

Figure 2. Reaction of $\approx 7\,\mathrm{cm}^3$ mercury contained in a 60 mm long stainless steel trough irradiated with a proton pulse of $20\mathrm{x}10^{12}$ 1 GeV protons. a) The height of the Hg-droplets obtained by image processing is averaged over ≈ 7 mm sections, 1.25 and 3.25 ms after proton impact. b) The computed [8, 9] energy deposition (asterisk) on beam axis of the proton pulse is compared to the initial velocities of the Hg-droplets (open circles). The predicted proportionality of the initial velocity to the temperature elevation is confirmed within the precision of the measurement.

Figure 3. Water vapour bubble collapsing close to the free surface. The velocity of the micro jet was not measured. A liquid dome is formed around the micro jet.

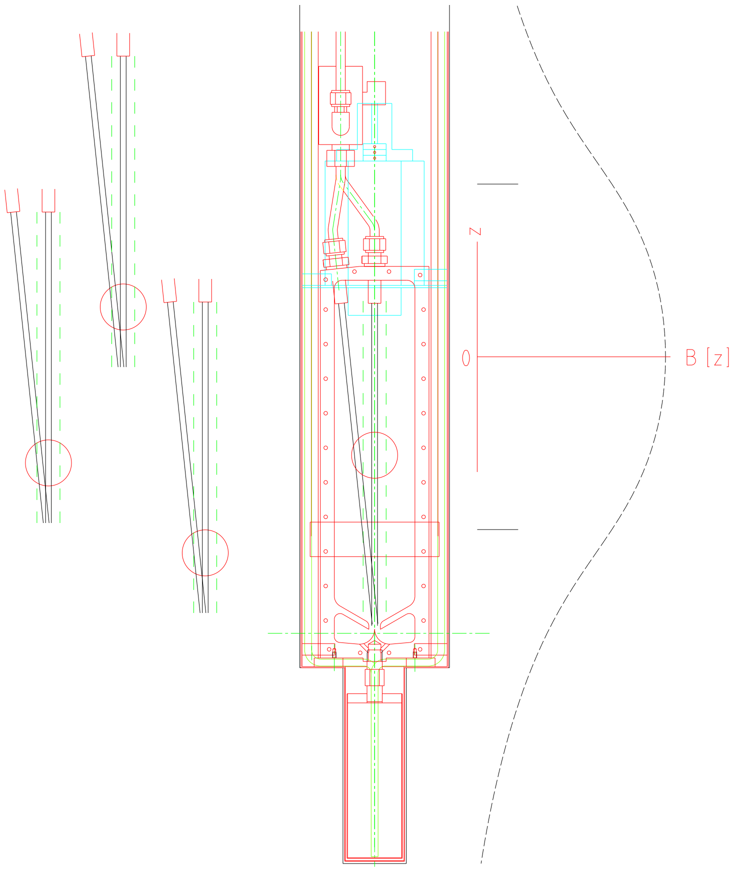

Figure 4. The experimental jet chamber placed in the M9 bore. Three positions of the experimental chamber within the magnet bore are indicated for both nozzles (coaxial, 6 degree injection). The circle indicates the effective size of the observation spot. These positions were dedicated to the observation of MHD effects in the maximum field gradients and in the homogeneous field region.

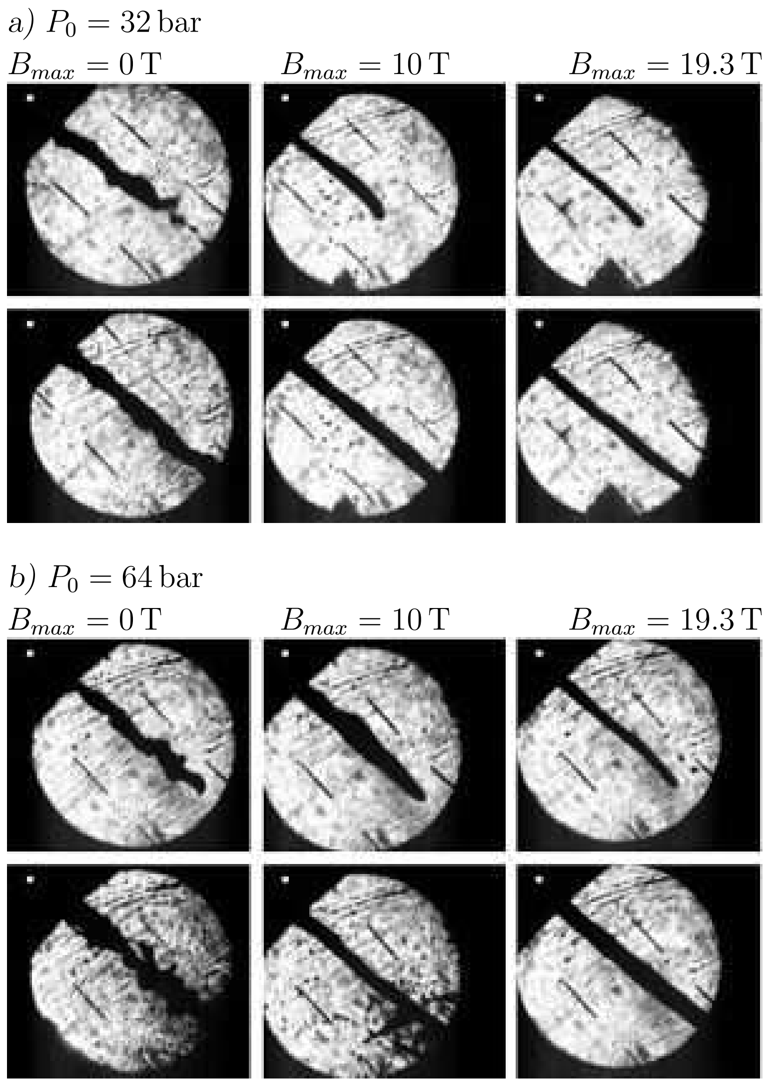

Figure 5. *Mercury jet injected at 6 degrees into the bore of the M9 magnet at GHMFL Grenoble. The tip of the jet is presented in the top row and the second row is a snap shot of the jet taken 10 ms after the passage of the tip. The static pressures driving the mercury were 32 (a) and 64 bars (b)*

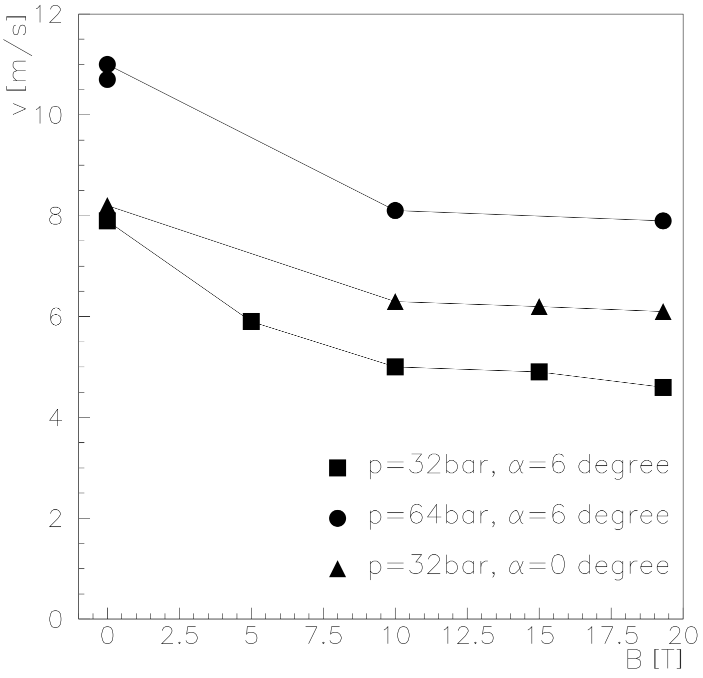

Figure 6. caption The velocity of the mercury jet as a function of the magnetic field shown at different initial static pressure and angles.